Invited Paper

Quantum networking with quantum dots coupled to micro-cavities

Edo Waks [a], Deepak Sridharan [a] and Jelena Vuckovic [b]

[a]IREAP, University of Maryland, College Park, MD, USa
[b]E.L. Ginzton Labs, Stanford University, Stanford, CA, USA

ABSTRACT

We describe an effect called Dipole Induced Transparency which enables a dipole emitter to strongly modify the cavity spectrum, even in the weak coupling regime. We then describe a method for generating entanglement and performing a full Bell measurement between two QDs using Dipole Induced Transparency. Finally, we show how DIT enables entanglement between QDs with vastly different radiative properties. The proposal is shown to be robust to cavity resonance mismatch.

Keywords: Entanglement, Quantum Dots, Quantum Optics

1. INTRODUCTION

The field of semiconductor cavity quantum electrodynamics (CQED) has seen rapid progress in the past several years. One of the main reasons for this is the development of high quality factors optical micro-cavities with mode volumes that are less than a cubic wavelength of light.[1] These high-Q cavities allow previously unattainable interaction strengths between a cavity mode and a dipole emitter such as a quantum dot.

There are a large number of applications that require strong interactions between a cavity and dipole emitter. These include methods for conditional phase shifts on single photons,[2] atom number detection,[3] and non-linear optics.[4] One important property of cavity-dipole interaction is that, under appropriate conditions, the dipole can flip the cavity from being highly transmissive to being highly reflective. This can result in entanglement between the dipole and reflected field. Such entanglement was used in reference[2] with a single-sided cavity configuration to achieve a quantum phase gate.

It has long been believed that in order for a dipole to fully switch the cavity, the vacuum Rabi frequency of the dipole, often denoted g, must exceed both the cavity and dipole decay rates. We refer to this regime as the high-Q regime. Here we show that in the "bad cavity" limit, defined as the regime where the cavity decay rate is much bigger than the dipole decay rate, the cavity can be switched almost perfectly, even when g is much smaller than the cavity decay rate. We consider a single cavity that is coupled to two waveguides and behaves as a resonant drop filter. Such systems are mathematically equivalent to driving a double-sided cavity with an incident field. The reflection properties of a single-sided cavity have been investigated elsewhere.[5] Drop filtering has been experimentally demonstrated in a variety of semiconductor systems including photonic crystals[6] and microdisks coupled to ridge waveguides.[7]

When an optical input field is resonant with the cavity, the drop filter would normally transmit all the field from one waveguide to another. Hence, the waveguide would appears opaque at the cavity resonance. We show that if one places a dipole in the drop-filter cavity, the waveguide becomes highly transparent even when g is much smaller than the cavity decay. In the high-Q regime this result is clear, because the cavity mode is split into a lower and upper polariton by more than a linewidth (normal modes splitting). In the low-Q regime, where g is less than the cavity decay rate, this result is surprising because the incident field can still drive both the cavity modes. Transparency in this regime is instead caused by destructive interference of the cavity field, which is analogous to the destructive interference of the excited state of a 3-level atomic system in Electromagnetically Induced Transparency (EIT).[8] For this reason we refer to this effect as Dipole Induced Transparency (DIT).

Further author information: (Send correspondence to E.W.)
E.W.: E-mail: edowaks@umd.edu

Quantum Communications Realized
edited by Yasuhiko Arakawa, Masahide Sasaki, Hideyuki Sotobayashi,
Proc. of SPIE Vol. 6780, 67800A, (2007) · 0277-786X/07/$18 · doi: 10.1117/12.732259

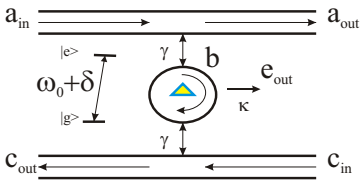

Figure 1. Cavity waveguide system for quantum repeaters.

The fact that switching can be observed without the high-Q regime is extremely important for the field of semiconductor CQED. Although the high-Q regime has been achieved in atom cavity QED,[3] it is extremely difficult to achieve using semiconductor technology. Semiconductor implementations of cavity QED systems, such as photonic crystal cavities coupled to quantum dots, usually suffer from large out-of-plane losses, resulting in short cavity lifetimes. Things become even more difficult when one attempts to integrate these cavities with waveguides. The cavity-waveguide coupling rate must be sufficiently large that we do not lose too much of the field out-of-plane. At the same time, leakage into the waveguide introduces additional losses making the high-Q regime even more difficult to achieve. Our result relaxes the constraint on using the high-Q regime, allowing complete switching in a more practical parameter regime for semiconductors. To demonstrate the application of DIT, we conclude this paper by showing how it can be used to share entanglement between spatially separated dipoles, and to perform a full non-destructive Bell measurement on two dipoles. These operations are extremely useful for building quantum repeaters.[9,10]

One of the primary challenges in building quantum repeaters using solid state emitters such as Indium Arsenide quantum dots is that no two QDs are the same. Inhomogeneous broadening due to size fluctuation and local strain environment create large variations in radiative properties. In the second part of the manuscript we describe how DIT can be used to overcome this limitation and entangle non-identical radiators.

2. DIPOLE INDUCED TRANSPARENCY

Fig. 1 shows a schematic of the type of system we are considering. A cavity containing a single dipole emitter is evanescently coupled to two waveguides. The cavity is assumed to have a single mode that couples only to the forward propagating fields. The dipole may be detuned by δ from cavity resonance, denoted ω_0, while g is the vacuum Rabi frequency of the dipole. Both waveguides are assumed to have equal coupling rate into the cavity. This condition is known as critical coupling, and results in the input field from one waveguide being completely transmitted to the other when $\gamma \gg \kappa$.[11]

We begin with the Heisenberg operator equations for the cavity field operator $\hat{\mathbf{b}}$ and dipole operator σ_-, given by[12]

$$\begin{aligned} \frac{d\hat{\mathbf{b}}}{dt} &= -\left(i\omega_0 + \gamma + \kappa/2\right)\hat{\mathbf{b}} - \sqrt{\gamma}\left(\hat{\mathbf{a}}_{in} + \hat{\mathbf{c}}_{in}\right) \\ &\quad -\sqrt{\kappa}\hat{\mathbf{e}}_{in} - ig\sigma_- \qquad (1) \\ \frac{d\sigma_-}{dt} &= -\left(i\left(\omega_0 + \delta\right) + \frac{1}{2\tau}\right)\sigma_- + ig\sigma_z\hat{\mathbf{b}} - \hat{\mathbf{f}} \qquad (2) \end{aligned}$$

The operators $\hat{\mathbf{a}}_{in}$ and $\hat{\mathbf{c}}_{in}$ are the field operators for the flux of the two input ports of the waveguide, while $\hat{\mathbf{e}}_{in}$ is the operator for potential leaky modes due to all other losses such as out-of-plane scattering and material absorption. The bare cavity has a resonant frequency ω_0 and an energy decay rate κ (in the absence of coupling to the waveguides). This decay rate is related to the cavity quality factor Q by $\kappa = \omega_0/Q$. The parameter γ is the energy decay rate from the cavity into each waveguide. Similarly, the dipole operator σ_- has a decay rate $1/2\tau$, and $\hat{\mathbf{f}}$ is a noise operator which preserves the commutation relation. The output fields of the waveguide, $\hat{\mathbf{a}}_{out}$ and $\hat{\mathbf{c}}_{out}$, are related to the input fields by $\hat{\mathbf{a}}_{out} - \hat{\mathbf{a}}_{in} = \sqrt{\gamma}\hat{\mathbf{b}}$ and $\hat{\mathbf{c}}_{out} - \hat{\mathbf{c}}_{in} = \sqrt{\gamma}\hat{\mathbf{b}}$.[12] Our analysis works in the weak excitation limit, where the quantum dot is predominantly in the ground state. In this limit, $\langle\sigma_z(t)\rangle \approx -1$ for all time, and we can substitute $\sigma_z(t)$ with its average value of -1.

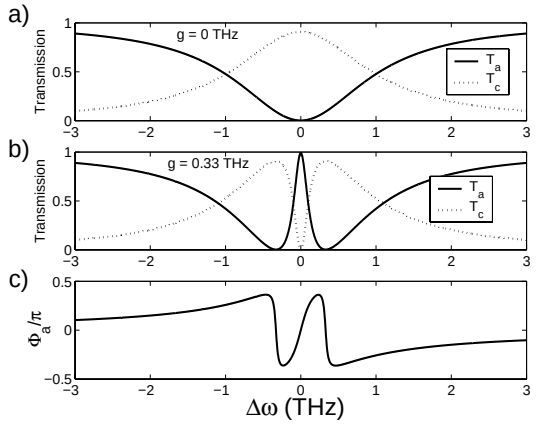

Figure 2. Probability for field in $\hat{\mathbf{a}}_{in}$ to transmit into $\hat{\mathbf{a}}_{out}$ and $\hat{\mathbf{c}}_{out}$ respectively. (a) transmission with no dipole in cavity. (b) transmission with a dipole in the cavity. c) Phase imposed on transmitted field when a dipole is present in the cavity.

Assuming the cavity is excited by a weak monochromatic field with frequency ω, we calculate the response of $\hat{\mathbf{b}}$ and σ_- in frequency space. We assume that the cavity decay rate is much faster than the dipole decay rate, so that $1/(\tau\gamma) \approx 0$. This is a realistic assumption for a quantum dot coupled to a photonic crystal cavity, but does not necessarily apply in atomic systems coupled to very high-Q optical resonators. In this limit the waveguide output can be solved and are given by:

$$\hat{\mathbf{a}}_{out} = \frac{-\gamma\hat{\mathbf{c}}_{in} + \left(-i\Delta\omega + \frac{\kappa}{2} + \frac{g^2}{-i(\Delta\omega-\delta)+1/2\tau}\right)\hat{\mathbf{a}}_{in} - \sqrt{\kappa\gamma}\hat{\mathbf{e}}_{in}}{-i\Delta\omega + \gamma + \kappa/2 + \frac{g^2}{-i(\Delta\omega-\delta)+1/2\tau}} \tag{3}$$

$$\hat{\mathbf{c}}_{out} = \frac{-\gamma\hat{\mathbf{a}}_{in} + \left(-i\Delta\omega + \frac{\kappa}{2} + \frac{g^2}{-i(\Delta\omega-\delta)+1/2\tau}\right)\hat{\mathbf{c}}_{in} - \sqrt{\kappa\gamma}\hat{\mathbf{e}}_{in}}{-i\Delta\omega + \gamma + \kappa/2 + \frac{g^2}{-i(\Delta\omega-\delta)+1/2\tau}} \tag{4}$$

where $\Delta\omega = \omega - \omega_0$.

Consider the case where the dipole is resonant with the cavity, so that $\delta = 0$. In the ideal case, the bare cavity decay rate κ is very small and can be set to zero. In this limit, when the field is resonant with the cavity and $g = 0$ we have $\hat{\mathbf{a}}_{in} = -\hat{\mathbf{c}}_{out}$, as one would expect from critical coupling. In the opposite regime, when $2\tau g^2 \gg \gamma + \kappa/2$ we have $\hat{\mathbf{a}}_{in} = \hat{\mathbf{a}}_{out}$, so that the field remains in the original waveguide. This condition can be re-written as $F_p = 2\tau g^2/(\gamma + \kappa/2) \gg 1$, where F_p is the Purcell factor. Thus, in order to make the waveguide transparent (i.e. decouple the field from the cavity), we need to achieve large Purcell factors. However, we do not need the full normal mode splitting condition $g > \gamma + \kappa/2$. When $1/\tau \ll \gamma + \kappa/2$ we can achieve transparency for much smaller values of g.

Fig. 2 plots the probability that $\hat{\mathbf{a}}_{in}$ transmits into $\hat{\mathbf{a}}_{out}$ and $\hat{\mathbf{c}}_{out}$. Assuming that the initial field begins in mode $\hat{\mathbf{a}}_{in}$, we define $\hat{\mathbf{a}}_{out}/\hat{\mathbf{a}}_{in} = \sqrt{T_a}e^{i\Phi_a}$ and $\hat{\mathbf{c}}_{out}/\hat{\mathbf{a}}_{in} = \sqrt{T_c}e^{i\Phi_c}$, and use cavity and dipole parameters that are appropriate for a photonic crystal cavity coupled to a quantum dot. We set $\gamma = 1THz$ which is about a factor of 10 faster than κ for a cavity with a quality factor of $Q = 10,000$. We set $g = 0.33THz$, a number calculated from FDTD simulations of cavity mode volume for a single defect dipole cavity in a planar photonic crystal coupled to a quantum dot.[1] The dipole decay rate is set to $1/\tau = 1GHz$, taken from experimental measurements.[13]

Panel (a) of Fig. 2 considers the case where the cavity does not contain a dipole. In this case $g = 0$, representing a system where two waveguides are coupled by a drop filter cavity, whose transmission width is determined by the lifetime of the cavity. When a dipole is present in the cavity, the result is plotted in panel (b). In this case, a very sharp peak in the transmission spectrum appears at $\Delta\omega = 0$, with a width of approximately 0.1THz. Because g is three times smaller than the cavity linewidth, this peak is not caused by normal mode splitting, but rather by destructive interference of the cavity field.

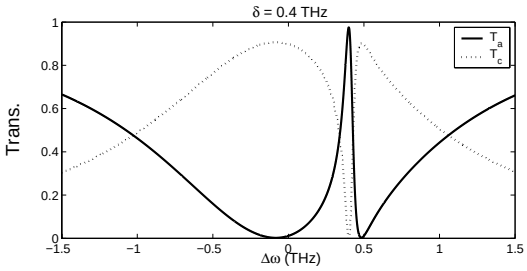

Figure 3. Transmission of waveguide for $\delta = 0.4Thz$, the detuning of the dipole from the cavity.

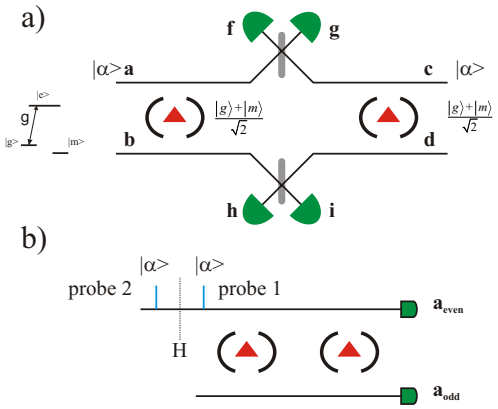

Figure 4. Application of DIT to quantum repeaters. a) a method for generating entanglement between two dipoles using DIT. b) a non-destructive Bell measurement.

In the bad cavity limit, where $1/\tau$ is very small, a simple expression for the width at full width half maximum of the dip can be calculated in the limit that $\gamma \gg \kappa/2$ (cavity losses are dominated by waveguides). In this limit, the width of the dip is found to be $\sqrt{\gamma^2 + 4g^2} - \gamma$. In the high-Q regime where $g \gg \gamma$, the transmission dip is equal to $2g$ as expected by normal mode splitting. In the low-Q regime where $g \ll \gamma$, the spectral width of the transmission peak is equal to $2g^2/\gamma = 2/\tau_{mod}$ (where τ_{mod} is the modified spontaneous emission lifetime of the dipole). This difference in functional behavior, i.e. quadratic vs. linear dependence in g, is indicative of the fact that transmission in the low-Q regime originates from a different physical process than the high-Q regime. The width of the transmission peak is important because it places a bandwidth limitation on the incoming pulse. In the low-Q regime, this bandwidth limitation means that the incoming pulse must be longer than the modified spontaneous emission lifetime of the dipole, while in the high-Q regime it must be longer then the Rabi oscillation period $1/g$.

In panel (c) we plot Φ_a for the case where $g = 0.33THz$. The region near zero detuning exhibits very large dispersion, which results in a group delay given by $\tau_g = (\gamma + \kappa/2)/g^2$. One can show that the group velocity dispersion at zero detuning vanishes, ensuring that the pulse shape is preserved.

We now consider the effect of detuning the dipole. The transmission spectrum for a dipole detuned by $\delta = 0.4Thz$ is plotted in Fig 3. Introducing a detuning in the dipole causes a shift in the location of the transmission peak, which occurs at the dipole resonant frequency. Thus, we do not have to hit the cavity resonance very accurately to observe DIT. We only need to overlap the dipole resonance within the cavity transmission spectrum.

3. QUANTUM NETWORKING USING DIT

The fact that we can switch the transmission of a waveguide by the state of a dipole in the low-Q regime can be extremely useful for quantum information processing. As one example, we now present a way in which DIT can be applied to engineering quantum repeaters for long distance quantum communication. Quantum repeaters can be implemented all optically,[14,15] as well as using atomic systems.[10] One of the main problems with these

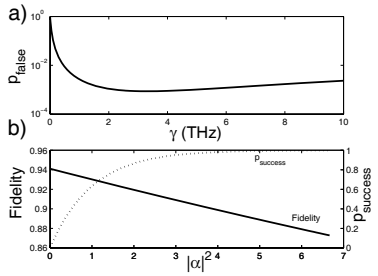

Figure 5. Panel (a), probability of detecting even parity for an odd parity state as a function of γ. Panel (b), solid line plots the fidelity of the state $(|gg\rangle \pm |mm\rangle)/\sqrt{2}$ after a parity measurement. Dotted line plots the probability that the measuring field contains at least one photon for detection.

proposals is that it is difficult to implement the full Bell measurement required for swapping entanglement. This leads to a communication rate that is exponentially decaying with the number of repeaters. More recent proposals incorporate interaction between nuclear and electron spins to implement the full Bell measurement.[16] Here we propose a method for implementing entanglement, as well as a full Bell measurement on an atomic system using only interaction with a coherent field. This leads to an extremely simple implementation of a quantum repeater.

In panel (a) of Fig. 4 we show how DIT can be used to generate entanglement between two spatially separated dipoles. A weak coherent beam is split on a beamsplitter, and each port of the beamsplitter is then sent to two independent cavities containing dipoles. The waveguide fields are then mixed on a beamsplitter such that constructive interference is observed in ports $\hat{\mathbf{f}}$ and $\hat{\mathbf{h}}$. Each dipole is assumed to have three relevant states, a ground state, an excited state, and a long lived metastable state which we refer to as $|g\rangle$, $|e\rangle$, and $|m\rangle$ respectively. The transition from ground to excited state is assumed to be resonant with the cavity while the metastable to excited state transition is well off resonance from the cavity, and is thus assumed not to couple to state $|e\rangle$. The states $|g\rangle$ and $|m\rangle$ represent the two qubit states of the dipole.

When the dipole is in state $|m\rangle$, it does not couple to the cavity, which now behaves as a drop filter. Thus, we have a system that transforms $\hat{\mathbf{a}}_{in}^{\dagger}|g\rangle|0\rangle \rightarrow \hat{\mathbf{a}}_{out}^{\dagger}|g\rangle|0\rangle$ and $\hat{\mathbf{a}}_{in}^{\dagger}|m\rangle|0\rangle \rightarrow -\hat{\mathbf{c}}_{out}^{\dagger}|m\rangle|0\rangle$. This operation can be interpreted as a C-NOT gate between the state of the dipole and the incoming light. When the dipole is in a superposition of the two states, this interaction generates entanglement between the path of the field and the dipole state. After the beamsplitter, this entanglement will be transferred to the two dipoles. If the state of both dipoles is initialized to $(|g\rangle + |m\rangle)/\sqrt{2}$, it is straightforward to show that a detection event in ports $\hat{\mathbf{g}}$ or $\hat{\mathbf{i}}$ collapses the system to $(|g,m\rangle - |m,g\rangle)/\sqrt{2}$.

Another important operation for designing repeaters is a Bell measurement, which measures the system in the states $|\phi_{\pm}\rangle = (|gg\rangle \pm |mm\rangle)/\sqrt{2}$ and $|\psi_{\pm}\rangle = (|gm\rangle \pm |mg\rangle)/\sqrt{2}$. Panel (b) of Fig. 4 shows how to implement a complete Bell measurement between two dipoles using only cavity waveguide interactions with coherent fields. The two cavities containing the dipoles are coupled to two waveguides. When a coherent field $|\alpha\rangle$ is sent down waveguide 1, each dipole will flip the field to the other waveguide if it is in state $|m\rangle$, and will keep the field in the same waveguide if it is in state $|g\rangle$. Thus, a detection event at ports $\hat{\mathbf{a}}_{even}$ and $\hat{\mathbf{a}}_{odd}$ corresponds to a parity measurement. A Bell measurement can be made by simply performing a parity measurement on the two dipoles, then a Hadamard rotation on both dipoles, followed by a second parity measurement. This is because a Hadamard rotation flips the parity of $|\psi_{+}\rangle$ and $|\phi_{-}\rangle$, but does not affect the parity of the other two states.

The performance of the Bell apparatus is analyzed in Fig 5. Panel (a) plots the probability that an odd parity state will falsely create a detection event in port $\hat{\mathbf{a}}_{even}$, as a function of γ. The probability becomes high at large γ due to imperfect transparency. It also increases at small γ because of imperfect drop filtering. The minimum value of about 10^{-3} is achieved at approximately 3THz. In panel (b) of Fig. 5 we plot both the fidelity and success probability of a parity measurement as a function of the number of photons in the probe field. The fidelity is calculated by applying the Bell measurement to the initial state $|\psi_i\rangle = (|g,g\rangle \pm |m,m\rangle)/\sqrt{2}$, and defining the fidelity of the measurement as $F = |\langle\psi_f|\ \psi_i\rangle|^2$, where $|\psi_f\rangle$ is the final state of the total system which includes the external reservoirs. The probability of success is defined as the probability that at least one photon is contained in the field. The fidelity is ultimately limited by cavity leakage, which results in "which

path" information beaing leaked to the environment. This information leakage depends the strength of the measurement which is determined by the number of photons in the probe fields. Using more probe photons results in a higher success probability, but a lower fidelity. To calculate this tradeoff, we use previously described values for cavity and reservoir losses, and set the coupling rate γ to 4THz, which is where the probability of false detection is near its minimum. At an average of three photons, a fidelity of over 90% can be achieved with a success probability exceeding 95%. These numbers are already promising, and improved cavity and dipole lifetimes could lead to even better operation.

4. ENTANGLING NON-IDENTICALLY EMITTING QDS

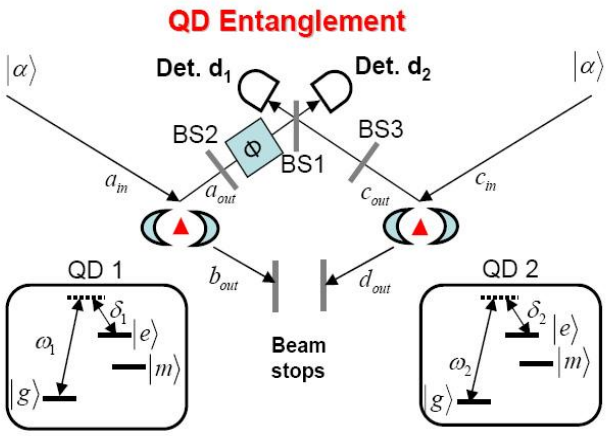

Figure 6. Schematic of cavity waveguide system for generating entanglement between two spatially separated dipoles using DIT

One of the main problems with generating entanglement between QDs is that they have vastly different frequencies and lifetimes. In this final section we show how DIT can be used to overcome this difficult limitation. The schematic for generating entanglement between two spatially separated non-identical quantum dots is shown in Figure 1. Each qubit consists of a quantum dot coupled to a double sided cavity. We define a_{in} and c_{in} as the two input modes to the cavity, and a_{out} and c_{out} as the reflected modes, and b_{out} and d_{out} as the transmitted modes. Each dipole is assumed to have three states: a ground state, a long lived metastable state and an excited state, which we refer to as $|g\rangle$, $|m\rangle$ and $|e\rangle$. The transition from the ground state to the excited state may be detuned by δ_1 and δ_2 from resonant frequencies of the two cavities , denoted by ω_1 and ω_2 respectively. The transition from the metastable state to the excited state is assumed to be decoupled from state $|e\rangle$ due to either spectral detuning or selection rules. The states $|g\rangle$ and $|m\rangle$ represent the two qubits of the system. The bare cavities have an energy decay rate of κ(in the absence of coupling to the waveguides) which is due to losses such as out-of-plane scattering and material absorption. The energy decay rates of the cavities into the reflected and transmitted modes are given by γ_1 and γ_2 respectively. The dipoles have a decay rate of $1/2\tau$.

The operators $\hat{\mathbf{a}}^\dagger_{in}$ and $\hat{\mathbf{c}}^\dagger_{in}$ are the bosonic creation operators for input flux in the top waveguide as indicated in Figure 1. They interact with the cavity-dipole system and transform the fields in the waveguide system according to the equations $\hat{\mathbf{a}}^\dagger_{out} = \mathrm{A}_g(\omega)\hat{\mathbf{a}}^\dagger_{in}$ and $\hat{\mathbf{c}}^\dagger_{out} = \mathrm{C}_g(\omega)\hat{\mathbf{c}}^\dagger_{in}$ where[12]

$$A_g(\omega) = \frac{(-i\Delta\omega_1 + \frac{\kappa}{2} + \frac{\gamma_2}{2} - \frac{\gamma_1}{2} + \frac{g^2}{-i(\Delta\omega_1 - \delta_1) + \frac{1}{2\tau}})}{(-i\Delta\omega_1 + \frac{\kappa}{2} + \frac{\gamma_2}{2} + \frac{\gamma_1}{2} + \frac{g^2}{-i(\Delta\omega_1 - \delta_2) + \frac{1}{2\tau}})} \tag{5}$$

$$C_g(\omega) = \frac{(-i\Delta\omega_2 + \frac{\kappa}{2} + \frac{\gamma_2}{2} - \frac{\gamma_1}{2} + \frac{g^2}{-i(\Delta\omega_2 - \delta) + \frac{1}{2\tau}})}{(-i\Delta\omega_2 + \frac{\kappa}{2} + \frac{\gamma_2}{2} + \frac{\gamma_1}{2} + \frac{g^2}{-i(\Delta\omega_2 - \delta) + \frac{1}{2\tau}})} \tag{6}$$

Equations 1 and 2 give the reflection of the waveguides when the dipoles are in the $|gg\rangle$ state. When the dipoles are in the $|mm\rangle$ state, they do not couple to cavities, and the reflection coefficients $A_m(\omega)$ and $C_m(\omega)$ are given by setting g = 0 in the above equations.

To understand how the protocol works, consider first the ideal case when the cavity resonant frequencies are the same and the dipoles are resonant with the cavities. Assume $\kappa = 0$ and $\gamma_1 = \gamma_2$. In this limit we have $A_g = C_g = F_p/(1 + F_p)$ and $A_m = C_m = 0$. The constant $F_p = 4g^2\tau/(\gamma_1 + \gamma_2)$ is called the Purcell factor. It is, in fact, the ratio of the cavity coupled dipole decay rate $2g^2/(\gamma_1 + \gamma_2)$ to the bare dipole decay rate $1/2\tau$. When $F_p >> 1$ we have $A_g = C_g = 1$. Thus, when the dipole is in state $|g\rangle$, the field is completely reflected and when it is in state $|m\rangle$, the field is completely transmitted.

The protocol work as follows. Both dipoles are initialized to be in an equal superposition of the dipole states $|g\rangle$ and $|m\rangle$. Thus, the initial state is given by $1/2(|gg\rangle + |mm\rangle + |gm\rangle + |mg\rangle)$. A weak coherent field $|\alpha\rangle$ with frequency ω_c (the resonant frequency of the cavity) is inserted at inputs a_{in} and c_{in}. The reflected field from the two cavities is mixed on a 50/50 beamsplitter, as shown in Fig. 1, and the phase ϕ is adjusted so the two fields constructively interfere at detector $\hat{\mathbf{d}}_1$. For the moment, ignore the presence of the beamsplitters BS2 and BS3, the role of these beamsplitters will become clear later. Now, if the dipoles are in the state $|mm\rangle$, both fields are transmitted at the cavities and dissipated at beam stops. Therefore, the state $|mm\rangle$ cannot produce a detection event at $\hat{\mathbf{d}}_1$ or $\hat{\mathbf{d}}_2$. Similarly, for the state $|gg\rangle$ both fields are completely reflected and constructively interfere at detector $\hat{\mathbf{d}}_1$. Only the states $|gm\rangle$ and $|mg\rangle$ can cause a detection event at state $\hat{\mathbf{d}}_2$. Using the coefficients in Eq. 1 and 2 in the idealized limit, we see that a detection event at detector $\hat{\mathbf{d}}_2$ collapses the state of the qubits to $(|gm\rangle - |mg\rangle)/\sqrt{2}$.

We define the efficiency of the protocol as the probability of detecting a photon at detector $\hat{\mathbf{d}}_2$ normalized by the field intensity $|\alpha|^2$. For the ideal case, efficiency is .125 as 50% of the field is lost when the dipoles are in states $|gg\rangle$ and $|mm\rangle$ for which we never get clicks at $\hat{\mathbf{d}}_2$, 50% of the field drops into the bottom waveguide and another 50% is lost in the beamsplitter BS1 which equally splits the fields between the ports $\hat{\mathbf{d}}_1$ and $\hat{\mathbf{d}}_2$. Now, consider what happens when the dipole frequencies are no longer equal. If the dipole transition frequencies are different, a detection event at $\hat{\mathbf{d}}_2$ does not leave the system in an entangled state. In this case we no longer have perfect DIT, and the fields reflected from the two cavities will have different amplitudes. This is illustrated in Fig 2a. where the reflectivity of a cavity for $\delta = 0$ and $\delta = 0.4$ THz are plotted. The difference in amplitude will result in imperfect destructive interference at the detector $\hat{\mathbf{d}}_2$. This means that there is some probability that state $|gg\rangle$ may cause a detection event at detector $\hat{\mathbf{d}}_2$, which leads to an imperfect entangled state. The state $|mm\rangle$, however, does not pose a problem as the field is transmitted to the bottom waveguide completely.

In order to regain perfect destructive interference at detector $\hat{\mathbf{d}}_2$, we need to make the field amplitudes on both sides of the beamsplitter equal. This is achieved by introducing a beamsplitter in the path of the waveguide as shown in Figure 1. If $|A(\omega)|^2 > |C(\omega)|^2$, we introduce a beamsplitter BS2 as shown in Figure 1 with transmission coefficient $|T_1(\omega)|^2 = |C(\omega)/A(\omega)|^2$. If $|A(\omega)|^2 < |C(\omega)|^2$, we introduce a beamsplitter BS3 in the path of signal on the right arm of the top waveguide with transmission coefficient $|T_2(\omega)|^2 = |A(\omega)/C(\omega)|^2$. A phase shift of $\phi(\omega) = \tan^{-1}(C(\omega)/A(\omega))$ is added in the path to make the phases on both sides equal. By this method of compensation, the resulting fields on both sides will be equal and would destructively interfere at $\hat{\mathbf{d}}_2$.

Using the above compensation scheme, a perfect Bell state is created for any dipole detunings δ_1 and δ_2. We pay a price however, through a reduction in efficiency. When the detunings are large, the dipoles are not resonant with the incident field $|\alpha >$, and therefore we achieve very weak DIT. This means that even when the dipole is in the state $|g\rangle$ most of the field is till transmitted through the cavity. Only a small fraction of the field is reflected and so the probability of detecting a dipole at detector $\hat{\mathbf{d}}_2$ is significantly reduced.

To understand the effect of dipole detuning on efficiency, we plot the calculated efficiency as a function of dipole detuning δ_2 in Fig. 2b. We use calculation parameters that are appropriate for InAs quantum dots coupled to photonic crystal defect cavities. For the calculations in the paper, we set $\gamma = 1$ THz and $\kappa = 0$. We set g = 0.33 THz for both the quantum dots, a value taken from finite difference time domain(FDTD) simulations of the cavity mode volume of a single defect photonic crystal cavity and the known oscillator strength of InAs QDs.[1] The dipole decay rate τ is set to 1 GHz, taken from experimental measurements.[13] For the values of γ, κ and

g, the Purcell factor is 218, which corresponds to a cavity reflectivity of 99.54% when the field is resonant with the dipole.

The incoming laser frequency is the common cavity resonant frequency ω_1. Efficiency is limited by the larger of the two, δ_1 or δ_2. In Fig. 2b, the efficiency is unchanged in the regions where $\delta_2 < \delta_1$. This is because it is limited by δ_1, which is kept fixed. This explains the flat-top appearance of the efficiency curve. One can see that useful efficiencies are achievable even when the two dipoles are significantly detuned from each other.

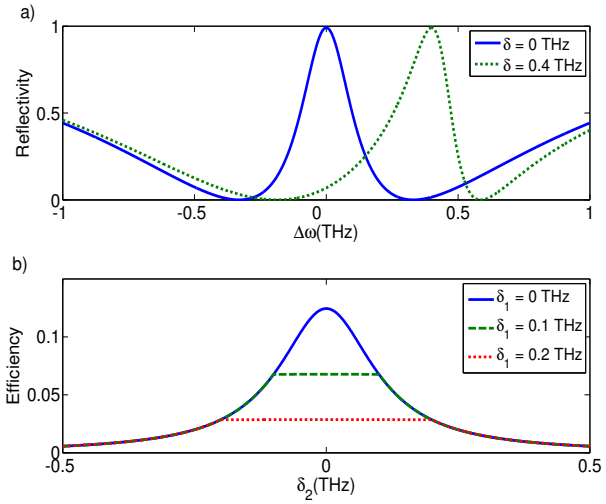

Figure 7. a) Reflectivity of a cavity for $\delta = 0$ and $\delta = 0.4$ THz b) Efficiency as a function of δ_2 when the cavity frequencies are the same ($\omega_1 = \omega_2$)

Now let's consider the case where the two cavities down's have the same resonant frequency. In this case, it is no longer clear which frequency we should use for the coherent field $|\alpha\rangle$. In general, this can depend on both the cavity separation and dipole detunings δ_1 and δ_2. Figure 3a plots the dependence of fidelity on the laser frequency for several different values of δ_1. The cavity separation $\Delta\omega_s = \omega_2 - \omega_1$ is set to 0.5 THz, and $\delta_2 = \Delta\omega_s/2$ (halfway between the frequencies of the two cavities). The value of the maximum fidelity, however, is the same for all three curves, and is given by 0.84. To understand why the maximum fidelity occurs at different frequencies but is independent of δ_2, we plot Figure 3b, the probabilities of photon detection at $\hat{\mathbf{d}}_2$ as a function of laser frequency when the dipoles are in the states $|gm\rangle$ and $|mg\rangle$ for $\delta_1 = 0.1$ THz and $\delta_2 = -0.3$ THz. The probability amplitudes for event detection at $\hat{\mathbf{d}}_2$ when the dipoles are in states $|gm\rangle$ and $|mg\rangle$ are denoted by $G_{gm}(w)$ and $G_{mg}(w)$ respectively. Similarly, we define $G_{gg}(w)$ and $G_{mm}(w)$ to be the magnitudes of field at $\hat{\mathbf{d}}_2$ when the dipoles are in the $|gg\rangle$ and $|mm\rangle$ states. If $|G_{gg}(w)|$ and $|G_{mm}(w)|$ are small, the final state of the system is approximately given by $(G_{gm}(w)|gm\rangle - G_{mg}(w)|mg\rangle)/\sqrt{|G_{gm}(w)|^2 + |G_{gm}(w)|^2}$, given there is a detection event at $\hat{\mathbf{d}}_2$. In order to have a maximally entangled state, $G_{gm}(w)$ should be equal to $G_{mg}(w)$. This happens at a unique frequency which depends on δ_1, δ_2, and the cavity detuning. At the optimal frequency, $G_{gg}(w)$ is equal to 0, as it is compensated for by the beamsplitters. $G_{mm}(w)$ remains almost a constant, since it is a strong function of cavity separation which does not change for the configuration. Fidelity is given by $(G_{gm}(w) + G_{mg}(w))/\sqrt{2(|G_{gm}|^2 + |G_{mg}|^2 + |G_{mm}|^2)}$, which is maximized when $G_{gm}(w)$ is equal to $G_{mg}(w)$. Hence, we always get a maximally entangled state at the frequency where fidelity is maximum. This frequency is referred to as the optimal frequency, ω_o. In Fig 3b, $\omega_o = 0.16$ THz. For every configuration of cavity resonant frequencies and dipole detunings, there is an optimal frequency where the fidelity is maximum and G_{gm} equals G_{mg}.

To understand the tradeoffs between peak fidelity and efficiency, Fig. 4a and 4b plot these two important parameters as a function of cavity detuning $\Delta\omega_s$, and dipole detuning δ_1. The variation in δ_1 is with respect

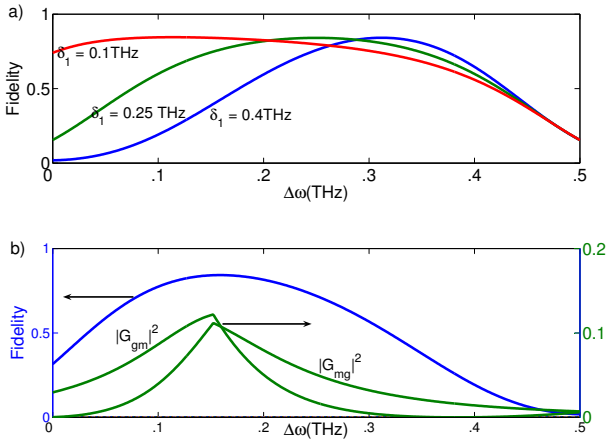

Figure 8. a)Fidelity as a function of frequency when δ_2 = -0.25 THz. The cavity separation is 0.5 THz b) Fidelity and probabilities of photon detection at $\hat{\mathbf{d}}_2$ as function of laser frequency. G_{gm} and G_{mg} are the probability amplitudes when the dipoles are in states $|gm\rangle$ and $|mg\rangle$

to the center frequency between the two cavities, denoted by $\omega_c = (\omega_1 + \omega_2)/2$. As Fig 4a shows, peak fidelity does not vary with dipole detuning. However, fidelity decreases with increase in cavity separation. A maximum fidelity of 1 achieved when the cavity separation is zero($\Delta\omega_s = 0$). In the limit that the cavity detunings are small relative to the cavity linewidth, we can derive an approximate expression for the fidelity which is given by $1/(1+3|A(\omega)|^2)$. For a cavity separation of 0.5 THz, this expression predicts a fidelity of 0.84 which is the same as the numerically calculated value shown in the figure. From Fig 4b, maximum efficiency of .125 is obtained for the most symmetric case i.e when the dipoles are located at the ω_c.

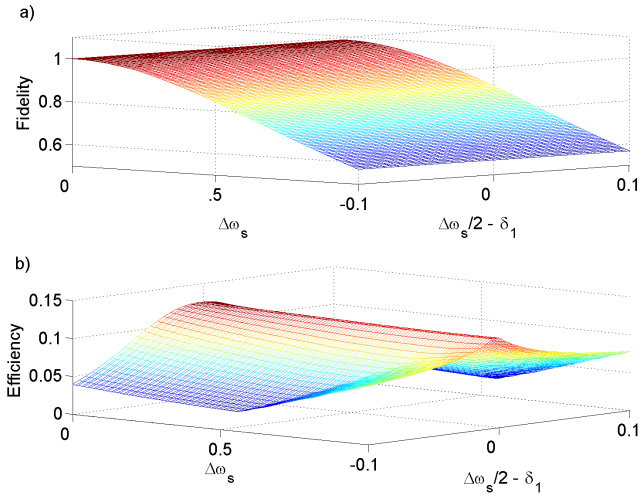

Figure 9. (a)(b) Fidelity and efficiency as a function of cavity separations $\Delta\omega_s$ and dipole detuning δ_1

So far we have always assumed that the cavity has an equal coupling rate to both waveguides, a condition known as critical coupling. We now consider the effect of adjusting the coupling rates. We will show that by properly adjusting these rates, we can compensate for the reduction in fidelity caused by cavity detuning. This allows us to achieve high fidelity when there is a mismatch between both dipoles and cavities.

The coupling rates of the waveguides into the cavities depend on the mode overlap between the two systems. This mode overlap can be adjusted by changing the distance between the two structures, and also by tuning the hole radii near the interaction region.

From the equations for $A(\omega)$ and $C(\omega)$, it is evident we can lump κ and γ_2 together into one parameter, $\gamma_t = \gamma_2 + \kappa$. We typically work in the regime where $\gamma_2 >> \kappa$, so the parameter γ_t can be tuned by changing γ_2. Figure 5 shows the dependence of fidelity and efficiency on the coupling rate of the cavities to the bottom waveguide γ_2 for three different δ_1s. Maximum efficiency of .5 is achieved when $\gamma_2 = 0$ which represents the case when the bottom waveguide is absent. This is sensible because light is never transmitted, so the probability of getting a detection at detector $\hat{\mathbf{d}}_2$ is increased. However, we also have low fidelity at this point because the state $|mm\rangle$ has a high probability of creating a detection event. As γ_t is increased, the efficiency decreases but the fidelity is increased. At a certain point, the fidelity reaches a peak value of 1, indicating the creation of an ideal Bell state. All previous calculations have worked in the regime where $\gamma_2 = \gamma_1$, but as the figure shows, this is not the ideal operating point. For each value of δ_1, there is a unique value for γ_t which achieves the optimal fidelity. This point can be better understood by considering the case when the cavities are separated by $\Delta\omega_s$ and the dipoles are located at $\Delta\omega_s/2$. For this symmetrical case, $|A_g(\omega)|$ and $|C_g(\omega)|$ are both equal, but there exists a phase difference between them. A change in γ_2 is equivalent to a change in the phase difference between the reflections from the cavities. For a particular value of γ_2, this phase difference is equal to the phase difference between $A_m(\omega)$ and $C_m(\omega)$. At this point the phase shifter compensates for both $|gg\rangle$ and $|mm\rangle$ and we never get clicks at $\hat{\mathbf{d}}_2$. There is a γ_2 for which $G_{mm}(w) = 0$ and hence fidelity is 1.

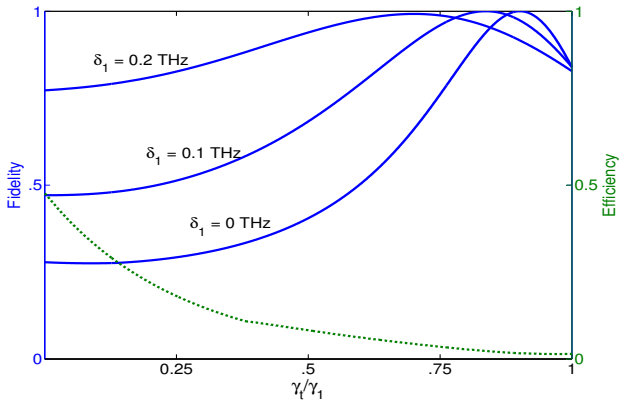

Figure 10. Fidelity and efficiency as a function of ratio of cavity-waveguide couplings(γ_t/γ_1)(Solid lines represent fidelity and the dotted line efficiency)

REFERENCES

1. J. Vuckovic and Y. Yamamoto, "Photonic crystal microcavities for cavity quantum electrodynamics with a single quantum dot," *App. Phys. Lett.* **82**(15), pp. 2374–2376, 2003.
2. L. M. Duan and H. J. Kimble, "Scalable photonic quantum computation through cavity-assisted interactions," *Phys. Rev. Lett.* **92**, p. 127902, 2004.
3. J. McKeever, J. R. Buck, A. D. Boozer, and H. J. Kimble, "Determination of the number of atoms trapped in an optical cavity," *Phys. Rev. Lett.* **93**, p. 143601, 2004.
4. Q. A. Turchette *et al.*, "Measruement of conditional phase shifts for quantum logic," *Phys. Rev. Lett.* **75**(25), pp. 4710–4713, 1995.
5. E. Waks and J. Vuckovic, "A full quantum repeater using dipole induced transparency." quant-ph/0510228.
6. H. Takano, B. Song, T. Asano, and S. Noda, "Highly efficient in-plane channel drop filter in a two-dimensional heterophotonic crystal," *App. Phys. Lett* **86**, p. 241101, 2005.

7. K. Djordjev, S. Choi, S. Choi, and P. D. Dapkus, "Microdisk tunable resonant filters and switches," *IEEE Photon. Technol. Lett.* **14**(6), pp. 828–830, 2002.
8. S. Harris, J.E.Field, and A. Imamoglu, "Nonlinear optical processes using electromagnetically induced transparency," *Phy. Rev. Lett.* **64**, pp. 1107–1110, 1990.
9. H. J. Briegel, W. Dür, J. Cirac, and P. Zoller, "Quantum repeaters: The role of imperfect local operations in quantum communication," *Phys. Rev. Lett.* **81**, pp. 5932–5935, December 1998.
10. Duan *et al.*, "Long-distance quantum communication with atomic ensembles and linear optics," *Nature* **414**(6862), pp. 413–418, 2001.
11. C. Manolatou *et al.*, "Coupling of modes analysis of resonant channel add-drop filters," *IEEE J. Quant. Electron.* **35**, p. 1322, September 1999.
12. D. Walls and G. Milburn, *Quantum Optics*, Springer, Berlin, 1994.
13. J. Vuckovic *et al.*, "Enhanced single photon emission from a quantum dot in a micropost microcavity," *App. Phys. Lett.* **82**, pp. 3596–3598, 2003.
14. Pan *et al.*, "Experimental entanglement purification of arbitrary unknown states," *Nature* **423**(6938), pp. 417–422, 2003.
15. E. Waks, A. Zeevi, and Y. Yamamoto, "Security of quantum key distribution with entangled photons against individual attacks," *Phys. Rev. A* **65**(4), p. 052310, 2002.
16. Childress *et al.*, "Fault-tolerant quantum repeaters with minimal physical resources, and implementations based on single photon emitters." quant-ph/0502112.